

## Temperature and magnetic field dependent optical spectral weight in the cation-deficient colossal-magnetoresistance material $\text{La}_{0.936}\text{Mn}_{0.982}\text{O}_3$

V. Golovanov and L. Mihaly

*Department of Physics, State University of New York at Stony Brook, Stony Brook, New York 11794-3800*

C. O. Homes

*Department of Physics, Brookhaven National Laboratory, Upton, New York 11973-5000*

W. H. McCarroll, K. V. Ramanujachary, and M. Greenblatt

*Department of Chemistry, Rutgers University, Piscataway, New Jersey 08854-8087*

(Received 26 May 1998)

The optical reflectivity of a vacancy doped colossal magnetoresistance material  $\text{La}_{0.936}\text{Mn}_{0.982}\text{O}_3$  has been investigated on single-crystal samples as a function of temperature and at zero and 0.5 T magnetic fields. The conductivity has been evaluated by Kramers-Kronig analysis in the frequency range of 100–20 000  $\text{cm}^{-1}$ . The broad peak in the optical conductivity, observed at room temperature around 10 000  $\text{cm}^{-1}$ , shifts towards zero as the ferromagnetic state develops at lower temperatures. In the transition regime the application of moderate magnetic field also induces a downward shift of the spectral weight. [S0163-1829(99)14401-1]

Reports on the colossal magnetoresistance (CMR) in La-A-MnO<sub>3</sub> compounds<sup>1–4</sup> (A = Ca, Sr, Ba) created renewed interest in the electric transport properties of the doped magnetic perovskites. The most prominent feature of this family of materials is that the ferromagnetic transition is accompanied by an insulator-to-metal transition in the electrical transport. It is well established that the electrical conductivity is sensitive to the magnetization of the sample and that, at temperatures close to the transition temperature, where the magnetization is strongly field dependent, CMR phenomenon is observed.

The “double-exchange” (DE) mechanism, where the Hund’s rule interaction between localized spins and mobile electrons hinders the electron hopping between misaligned magnetic sites, was suggested to explain the magnetoresistance in ferromagnetic perovskites.<sup>5</sup> More recently, Millis *et al.* pointed out that the DE arguments cannot explain the full magnitude of the observed MR in the manganates, and they suggested that the Jahn-Teller distortion of the MnO<sub>6</sub> octahedra plays an important role in the process.<sup>6</sup> In the structurally and magnetically similar cobaltates (like  $\text{La}_{1-x}\text{Sr}_x\text{CoO}_3$ ), where the occupation of the electronic orbitals is different from that of manganates, and which does not support a Jahn-Teller effect, the magnetoresistance is indeed much smaller.<sup>7,8</sup> By now there is an increasing amount of evidence supporting this model.<sup>9–14</sup>

The optical properties provide a valuable insight to the mechanism of the conductivity and to the CMR. The change of dc conductivity at the insulator-to-metal transition,<sup>2</sup> together with general arguments based on the oscillator sum rule, suggest that in the insulating state the spectral weight of the optical conductivity  $\sigma_1$  moves to nonzero frequencies. There are two different qualitative ways, with two entirely different underlying physical pictures, for the dc and optical conductivity to develop. It is possible that the conductivity peak at finite frequency gradually decreases in intensity, with no significant change in the characteristic frequency, whereas

a Drude-like peak grows at zero frequency. Alternatively, the finite frequency peak can move towards zero, developing a dc component in the process. The first process would correspond to “liberating” bound charges (as in the case of thermal excitations in semiconductors); the second one points to a more collective behavior. On the level of model calculations each one of these behaviors has been predicted (Refs. 15 and 16, respectively).

In accordance with the general arguments, a broad peak has been observed in  $\sigma_1$  various Mn-based CMR materials by several groups around 5000–9000  $\text{cm}^{-1}$ .<sup>14,17–20</sup> However, many of the experiments could not address crucial details of the spectral features, in particular the energy range which should be considered for the oscillator sum rule to be valid. The goal of the present study was threefold. First, taking advantage of the excellent sample quality, we wanted to reproduce and improve on the earlier optical conductivity studies in the metallic as well as in the insulating state. Second, we studied the transfer of spectral weight in the temperature range close to the transition temperature. Finally, we also investigated the effect of moderate magnetic field on the optical conductivity. Our main findings are the observation of the gradual shift of the prominent peak in  $\sigma_1$  towards zero frequency as the temperature is lowered across the transition, and a similar shift, induced by the application of the magnetic field. We also found that the integrated spectral weights of the high and low-temperature phases were different for energies up to 2 eV.

The single-crystal sample used on this study was grown by electrolysis of a melt obtained from mixtures of predried  $\text{Cs}_2\text{MoO}_4$  and  $\text{MoO}_3$  to which  $\text{MnCO}_3$  and  $\text{La}_2\text{O}_3$  were added. Electrolysis was carried out in air using Pt electrodes at temperatures in the range 975–1000 °C. Yttria-stabilized zirconia crucibles were used to contain the melt. When the electrolyses were carried out using a current of 10–15 mA for four-to-five days, black crystals of a cubiclike habit up to 3–5 mm were obtained. The crystals were mechanically

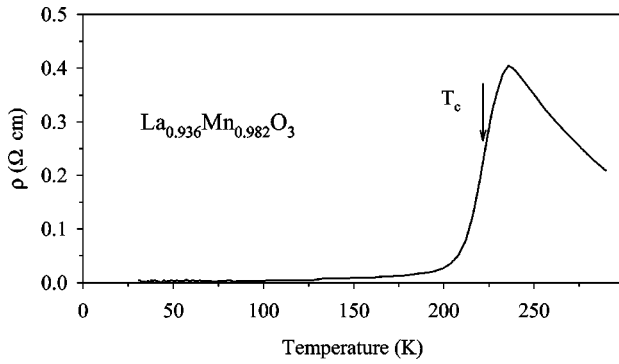


FIG. 1. The temperature dependence of the electrical resistivity, measured on a single-crystal sample from the same batch as the sample used in the optical study.

separated from the anode and subsequently washed with a warm solution of dilute  $K_2CO_3$  containing a small amount of disodiummethylenediaminetetraacetic acid. Chemical analysis for La and Mn contents were made with a Baird Atomic Model 2070 inductively-coupled-plasma emission spectrometer. Cs analysis was carried out by atomic absorption spectrometry.<sup>21</sup>

The electrical resistivity measurements were made with a closed-cycle refrigeration system in a four-probe configuration down to 30 K. The temperature-dependent resistivity (Fig. 1) shows typical metal-insulator transition, accompanied by magnetic ordering,<sup>21</sup> at  $T_c=225$  K with the peak value of resistivity ( $0.4 \Omega \text{ cm}$ ) being about twice higher than the room-temperature value. The magnetoresistance ( $[R(H=0) - R(H=5 \text{ T})]/R(H=0)$ ) has a peak value of 0.77. More details of the sample preparation and characterization are reported in Ref. 21.

Reflectivity measurements were performed in nearly normal incidence configuration using a Bomem-155 FTIR spectrometer ( $500\text{--}12\,000 \text{ cm}^{-1}$ ) and a Bruker 66v instrument ( $100\text{--}700 \text{ cm}^{-1}$ ) for  $80\text{--}300$  K temperature interval. The data in visible frequency range up to  $23\,000 \text{ cm}^{-1}$  at room temperature and up to  $16\,000 \text{ cm}^{-1}$  at 80 K was taken in the Bruker 66v. The surface of the as-grown crystal was smooth and shiny and did not require any additional treatment. In the Bomem spectroscope the sample was mounted with the shiny surface against a conical hole which determined the surface area exposed to the light. In the absence of the sample the reflectivity signal was checked to be zero. The background was taken by replacing the sample with a gold mirror. The measurements were first taken in zero magnetic field, then repeated in a magnetic field produced by a pair of Hicorex-Nd permanent magnets placed close to the sample. The field was perpendicular to the light incidence plane; the magnitude of the field at the sample position was measured to be 0.5 T. In the Bruker 66v the measurement was done with the overfilling technique:<sup>22</sup> the sample was mounted on the tip of a cone, background was taken by Au or Al evaporation on the sample surface.

The reflectivity (Fig. 2) shows almost no temperature dependence above  $T_c$  and a dramatic increase right below the transition temperature in the frequency range up to  $8\,000 \text{ cm}^{-1}$ . The inset illustrates the very sharp onset of metallic reflectivity at  $850 \text{ cm}^{-1}$ . Unlike in other CMR (doped) materials,<sup>17</sup> in our raw data there is a distinct separation

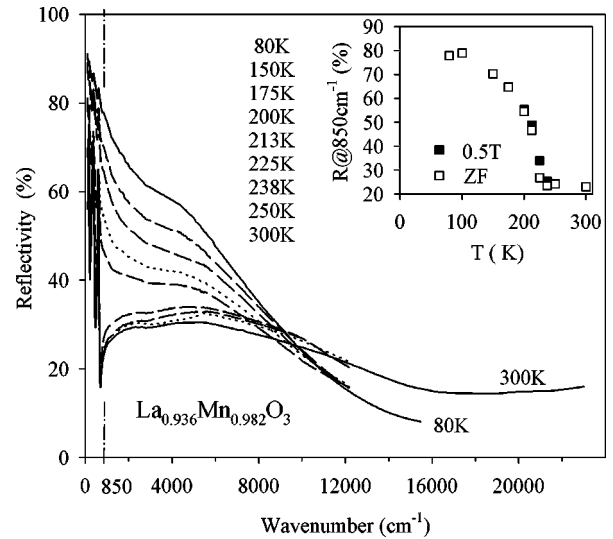


FIG. 2. Optical reflectivity at various temperatures. Curves are labeled from top to bottom at  $4000 \text{ cm}^{-1}$ . The inset shows the temperature dependence of the reflectivity at  $850 \text{ cm}^{-1}$  at zero magnetic field and at 0.5 T field. The optical analog of the CMR effect is apparent in the data around the transition temperature.

between the insulating and the metallic states. Moderate magnetic field of 0.5 T (Fig. 4) increases the low-frequency reflectivity in a narrow (10 K) temperature interval around  $T_c$ , the maximum effect is right at the transition temperature  $T=225$  K.

To obtain optical conductivity (Figs. 3, 4) Kramers-Kronig analysis of the data was performed. In order to complete the frequency range from zero to infinity, low- and high-frequency tails were added to each reflectivity curve. The calculated conductivity proved to be insensitive to the

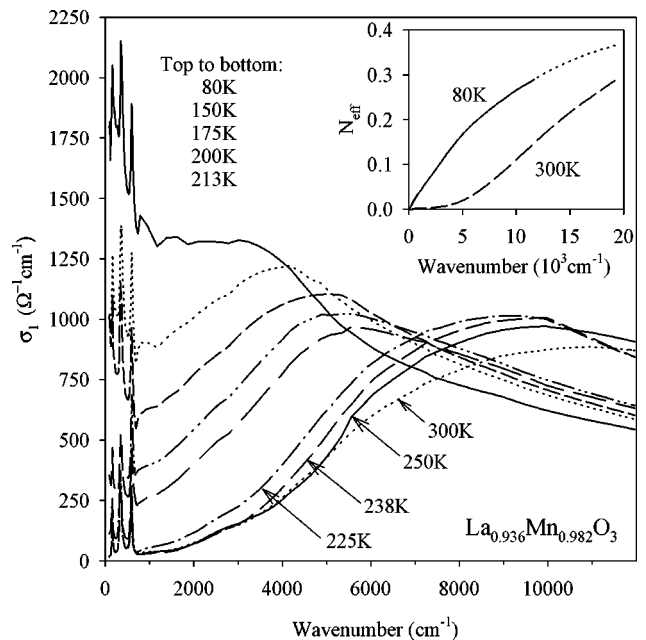


FIG. 3. Optical conductivity of the sample at various temperatures. Curves are labeled from top to bottom at  $4000 \text{ cm}^{-1}$ . The inset shows the integrated spectral weight, converted to effective electron number per formula unit  $N_{\text{eff}}$  by using the free-electron mass.

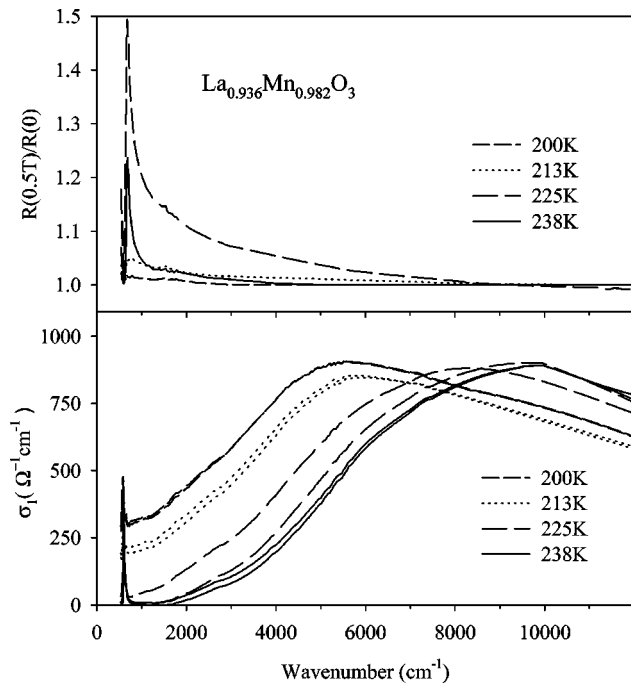


FIG. 4. Temperature development of the optical conductivity around the ferromagnetic transition (lower panel). Also shown are the effect of the magnetic field in terms of the reflectivity ratio (in 0.5 T relative to zero field, upper panel) and in the optical conductivity (for each of the two lines representing the same temperature the one that appears “shifted” to lower frequencies corresponds to in-field data).

exact shape of the low-frequency tail. At room-temperature above  $23\,000\text{ cm}^{-1}$  up to  $2.9 \times 10^5\text{ cm}^{-1}$  (36 eV) the reflectivity of the pure compound was used<sup>20</sup> and a  $1/\omega^4$  free-electron fit completed the range. Alternatively, we used the combined reflectivity curve of the doped compound<sup>17</sup> below 10 eV and that of the pure compound above. Below  $12\,000\text{ cm}^{-1}$  the difference between these two fits is insignificant. The conductivity reported here (Fig. 3) was obtained using the combined fit. Based on Ref. 17 it was assumed that there is no temperature dependence of reflectivity above  $30\,000\text{ cm}^{-1}$  and the reflectivity curves were smoothly merged to the room-temperature curve. The exact shape of this merge had little influence on conductivity below  $10\,000\text{ cm}^{-1}$ .<sup>23</sup>

The optical conductivity above  $T_c$  shows a broad peak centered at around  $10\,000\text{ cm}^{-1}$ . At temperatures around  $T_c$  the peak shifts to lower frequencies (Fig. 4). Even well below the transition, when the dc conductivity is fully developed, there is a peak in the optical conductivity (Fig. 3). The inset in Fig. 3 illustrates that the low-frequency spectral weight is much larger in the metallic state, and the difference of the spectral weights persists well above 1 eV ( $8000\text{ cm}^{-1}$ ).

The results reported here are in qualitative agreement with the calculations of Millis, Mueller, and Shraiman.<sup>16</sup> The main ingredients of the model are the electron hopping, the coupling between the conduction electrons and core electron spins (Hund’s coupling), the electron phonon coupling and the energy associated with the Jahn-Teller (JT) distortion, characterized by the parameters,  $t$ ,  $J$ ,  $g$ , and  $k$ , respectively. In the large- $J$  limit the behavior of the system is governed by

the dimensionless coupling constant  $\lambda = g^2/(tk)$ . The  $\lambda = 0$  case corresponds to the traditional DE model.<sup>24</sup> In Ref. 16 the Coulomb energy cost of having two  $e_g$  electrons on the same Mn site ( $U$ ) was neglected, and most of the calculations were performed for the case of one  $e_g$  electron per Mn site (“half-filled band”). The authors argued that the underlying physics is similar to that of a more realistic picture, where the band is less than half filled, and  $U$  is in fact very large. Recently, the model was further developed and applied to optical data on hole-doped manganates.<sup>14</sup>

Based on these ideas, we will interpret our results in a model where  $U$  and  $J$  are large and the band is less than half filled. The broad peak in the optical conductivity of the insulating sample is related to the transitions between a Jahn-Teller split (occupied) site and unsplit (empty) site. The excitation energy scales with the Jahn-Teller splitting of the  $e_g$  levels, and the wide distribution of energies results in a broad resonance feature. In the magnetically ordered state the  $e_g$  electrons are delocalized, the JT splitting is uniform and its magnitude is suppressed. A partially filled (i.e., less than one electron per site) band is formed from the degenerate nearest-neighbor sites. The dc conductivity is due to electrons in this band. As long as the JT splitting is finite, a finite frequency “resonant” transition is also possible, from the lower JT level to the neighboring higher JT level. In the metallic phase this transition is responsible for the upward trend in  $\sigma(\omega)$  at low frequencies, and for the broad peak around  $3500\text{ cm}^{-1}$ .

One of the important results of our experiment is the deficiency in spectral weights extending above 1 eV, similar to Refs. 18,19. In the framework of the interpretation outlined above, the energy range of our measurement includes the dc transport and also the JT splitting energies, but does not include the energy required for having an electron with the wrong spin direction ( $J$ ), or the energy of having two  $e_g$  electrons on the same site ( $U$ ). The conductivity spectral weight is, under quite general circumstances, proportional to the kinetic energy of the electrons,<sup>25</sup> i.e., the bandwidth. For processes extending up to 1 eV, the main difference between the magnetically ordered and disordered states is that the probability of nearest-neighbor jumping transition is reduced by spin disorder. The smaller hopping probability means reduced bandwidth, leading to reduced kinetic energy and smaller spectral weight.

In summary, we measured the optical conductivity over a wide range of frequencies on a high quality, vacancy doped crystal of the prototype CMR material. The electronic excitations as a function of frequency and magnetic field were studied, and qualitative understanding of the results was developed, using the theory of Millis and co-workers. Measurements at lower energies, covering the vibrational frequencies, are planned to explore the connection between lattice and electronic modes further.

The authors wish to thank P. B. Allen for many enlightening discussions. Work at SUNY, Stony Brook, was supported by the NSF Grant No. DMR-93-21575 Work at BNL was supported by the US Department of Energy, Division of Materials Science, under Contract No. DE-ACO2-98CH10886. The work at Rutgers University was supported by the NSF Solid State Chemistry Grant No. DMR-96-13106.

- <sup>1</sup>R. von Helmolt, J. Wecker, B. Holzapfel, L. Schultz, and K. Samwer, Phys. Rev. Lett. **71**, 2331 (1993).
- <sup>2</sup>A. Urushibara, Y. Moritomo, T. Arima, A. Asamitsu, G. Kido, and Y. Tokura, Phys. Rev. B **51**, 14 103 (1995).
- <sup>3</sup>S. Jin, T. H. Tiefel, M. McCormack, R. A. Fastnacht, R. Ramesh, and L. H. Chen, Science **264**, 413 (1994).
- <sup>4</sup>P. Schiffer, A. P. Ramirez, W. Bao, and S.-W. Cheong, Phys. Rev. Lett. **75**, 3336 (1995).
- <sup>5</sup>C. Zener, Phys. Rev. **82**, 403 (1951); P.-G. de Gennes, Phys. Rev. **118**, 141 (1959).
- <sup>6</sup>A. J. Millis, P. B. Littlewood, and B. I. Shraiman, Phys. Rev. Lett. **74**, 5144 (1995).
- <sup>7</sup>M. A. S  nar  s-Rodr  guez and J. B. Goodenough, J. Solid State Chem. **118**, 323 (1995).
- <sup>8</sup>V. Golovanov, L. Mihaly, and A. Moodenbaugh, Phys. Rev. B **53**, 8207 (1996).
- <sup>9</sup>C. H. Chen and S.-W. Cheong, Phys. Rev. Lett. **76**, 4042 (1996).
- <sup>10</sup>P. G. Radaelli, D. E. Cox, M. Marezio, and S.-W. Cheong, Phys. Rev. B **55**, 3015 (1997).
- <sup>11</sup>D. Louca, T. Egami, E. L. Brosha, H. Roder, and A. R. Bishop, Phys. Rev. B **56**, R8475 (1997).
- <sup>12</sup>G. Sub  as, J. Garc  a, J. Blasco, and M. G. Proietti, Phys. Rev. B **57**, 748 (1998).
- <sup>13</sup>C. H. Booth, F. Bridges, G. H. Kwei, J. M. Lawrence, A. L. Cornelius, and J. J. Neumeier, Phys. Rev. B **57**, 10 440 (1998).
- <sup>14</sup>M. Quijada *et al.*, cond-mat/9803201 (unpublished).
- <sup>15</sup>P. E. deBrito and H. Shiba, Phys. Rev. B **57**, 1539 (1988).
- <sup>16</sup>A. J. Millis, R. Mueller, and B. I. Shraiman, Phys. Rev. B **54**, 5405 (1996).
- <sup>17</sup>Y. Okimoto, T. Katsufuji, T. Ishikawa, A. Urushibara, T. Arima, and Y. Tokura, Phys. Rev. Lett. **75**, 109 (1995).
- <sup>18</sup>Y. Okimoto, T. Katsufuji, T. Ishikawa, T. Arima, and Y. Tokura, Phys. Rev. B **55**, 4206 (1997).
- <sup>19</sup>S. G. Kaplan, M. Quijada, H. D. Drew, D. B. Tanner, G. C. Xiong, R. Ramesh, C. Kwon, and T. Venkatesan, Phys. Rev. Lett. **77**, 2081 (1996).
- <sup>20</sup>T. Arima and Y. Tokura, J. Phys. Soc. Jpn. **64**, 2488 (1995).
- <sup>21</sup>W. H. McCarroll, K. V. Ramanujachary, M. Greeblatt, and F. Cosandey, J. Solid State Chem. **136**, 322 (1998).
- <sup>22</sup>C. C. Homes, M. Reedyk, D. A. Crandles, and T. Timusk, Appl. Opt. **32**, 2976 (1993).
- <sup>23</sup>We emphasize that the optical conductivity features discussed here are robust and they are not the artifacts of the evaluation processes. For a different high frequency tail used (still no temperature dependence above  $30\,000\text{ cm}^{-1}$  and a  $1/\omega^4$  cutoff starting at  $50\,000\text{ cm}^{-1}$ ), all these features and their relative positions were unchanged. The different tail caused the characteristic frequencies to shift downward.
- <sup>24</sup>K. Kubo and A. Ohata, J. Phys. Soc. Jpn. **33**, 21 (1972); N. Furukawa, *ibid.* **63**, 3214 (1994).
- <sup>25</sup>A. J. Millis and S. N. Coppersmith, Phys. Rev. B **42**, 10 807 (1990).